Construction and Excavation by Collaborative Double-Tailed SAW Robots

Luyang Robby Huang[1]*, Alexander Zhu[1]*, Kathleen Wang[1], Daniel I. Goldman[2], Andy Ruina[1], and Kirstin H. Petersen[1]

***Abstract*—We describe a minimalistic robot mechanism that is capable of many construction behaviors in dry granular material including locomotion, climbing, leveling, subtraction, addition, transport, and burrowing. The design extends upon a single-actuator wave mechanism with the insight that the tails can be used both for locomotion in and manipulation of granules. For simplicity, experiments are limited to 2 manually controlled or 2 open loop robots operating in a quasi-2D vertical arena filled with packing peanuts. We demonstrate and characterize construction by single- and multi-robot systems, with special attention to how mechanism improvement, autonomy, and 3D operation could be achieved. Remarkably, we find that the majority of behaviors are robust – that is, the robots can achieve the intended functionality through open loop control, largely eliminating the need for sophisticated perception. The experiments indicate an unprecedented, simple robotic solution to many of the classic challenges in autonomous construction.**

***Index Terms*—Biologically-Inspired Robots, Climbing Robots, Cooperating Robots, Robotics and Automation in Construction**

I. Introduction

ROBOTS capable of advanced interaction with granules may locomote through and build reinforcing structures in rubble during search and rescue, traverse unstructured terrain for remote-access exploration, place subterranean cables and sensors with minimal disruption, and construct access structures on extraterrestrial planets [1]. State of the art robots have prompted a wealth of point solutions to many of these challenges, relying e.g. on wheels and tracks [2], [3], legs [4], and peristalsis [5] for *locomotion*; root-like growth [6], [7], screws [8], [9], scoops [10] and bucket drums [11] for *excavation and burrowing*; and end effectors like grippers [12], [13] and scoops [14], [10] for *construction*, often combined with careful perception and planning[15], [16]. Few address multiple construction challenges, and even fewer permit multiple, mobile robots to collaborate in shaping the granular material[17], [18], [1]. Here, we present a simple 2-DOF robot mechanism that can locomote in, manipulate, excavate, and burrow into granular material as well as collaborate physically with other robots. Our solution is based on physical interactions between double-tailed "Single" Actuator Wave (SAW) robots. We show the construction repertoire of a single robot and how physical collaboration of two such robots unlocks a much richer set of construction behaviors.

SAW robots [19] are 1-DOF mechanisms consisting of a rectangular chain surrounding a helix that rotates around its own axis to produce a sinusoidal profile. The continuously propagating wave causes the links in the chain to effectively walk over the surface (Fig. 1.A), leveraging an isotropic coefficient of friction (opposite the anisotropic serpentine motion of snakes). Rotating the helix in the opposite direction prompts reverse motion. Despite the extreme simplicity of this mechanism, it has been demonstrated to move in a variety of terrains, in water, between constrained surfaces, and in flexible tubes[19]. Furthermore, it does not suffer from the risk of tangling and jamming in the same way as tracks which are the prototypical solution to motion on granular surfaces. Later iterations of the SAW design leveraged four actuators, a two-part helix with heads located at either end, and a symmetrical layout to enable climbing and steerable motion in any orientation [20].

To extend this robot design to work with granular media, we modified the design to consist of a single, low profile "head" which holds two motors and electronics and is located in the middle of two extruding helices ("tails") as shown in Fig. 1. This seemingly small modification has strong implications for robot-granule and robot-robot interactions. By rotating the two helices in the same direction the robot can move forward or backward; if the helices spin opposite each other, the robot stands still and either propels material outwards or inwards; finally, a stationary helix can act as an anchor to keep the robot stationary, while the other manipulates granules. The fact that the drive has a small form factor and is in line with the two helices, means that two robots can climb over each other and therefore interact closely in the same environment.

We first introduce the double-tailed design that permits two robots to climb over each other, then demonstrate and characterize their individual and collective ability to inter-

Figure 1. Untethered, double-tailed SAW robot on granules.

Manuscript received: September, 9, 2021; Revised December, 8, 2021; Accepted January, 5, 2022.

This paper was recommended for publication by Editor Clement Gosselin upon evaluation of the Associate Editor and Reviewers' comments.

This work was supported by a Cornell ELI grant, NSF CAREER grant #2042411, NSF grant #1933283, GETTYLABS, and a Packard Fellowship for Science and Engineering.

*The first two authors contributed equally to this work.

[1]College of Engineering, Cornell University, Ithaca, NY 14853, USA. <lh749> , <ayz8>, <kw456>, <ruina>, <kirstin> @cornell.edu, [2]School of Physics, Georgia Institute of Technology, Atlanta GA 30332, USA. daniel.goldman@physics.gatech.edu

Digital Object Identifier (DOI): see top of this page.

act with and modify their environment through leveling, constructing, excavating, transporting and burrowing. We restrict our proof-of-concept to a quasi-2D environment using packing peanuts as granules. Our system consists of two tethered, manually controlled robots, and two untethered robots operated open loop. We list distinct control sequences related to each behavior and discuss features important to future autonomous operation. The fact that most behaviors are achievable with open loop control is promising, in that it shows that these operations are relatively robust and will not require advanced feedback or sensing capabilities in future autonomous systems. Finally, we hint at simple ways in which the mechanism could be improved and how the system could be extended to 3D. We encourage the reader to watch the accompanying video (https://bit.ly/33uMwGN).

II. MECHANISM DESIGN

The double-tailed SAW robot is composed of one head, two 6V high power 380:1 Pololu Micro Metal Gear motors with magnetic encoders, two helices, two tail caps, and twenty four links. All mechanical components were 3D printed on low-end filament printers (Prusa mkII and Ender) using polylactic acid (PLA) and assembled using 3-48 nuts and bolts (Fig. 2). The head houses driver electronics and motors. A special link connects the tails to the head and helps transition the helix to the motor. The tail caps act both as a shovel allowing the robot to scoop, dig, and deposit material, and as a ramp enabling one robot to climb on top of another. Set screws attach the helices to the motors and the motors to the head. Finally, the robot is covered in stretchy fabric that prevents links from entangling when two robots interact.

In our trials, two parameters had significant effects. By increasing the ratio of the helix amplitude to period, the robot can climb larger obstacles at the cost of increasing the link-helix friction. In our implementation, the motor stall torque was exceeded at ratios above $\sim$0.25; for safety, we used $\sim$0.17. The second key parameter is the size of the head, which acts as a "dead zone" where the robot only passively interacts with granules. In our design, the head length is similar to the length of the motor (32mm), and roughly the same as the links. By nesting the head between the two helices, the robot is able to manipulate material and climb onto other robots in both directions.

We mounted a 3.7V 220mAh LiPo battery and a custom printed circuit board on the head. The board has an ItsyBitsy M0 Express controller, a buck-boost regulator (MC34063ACD), and a dual motor driver (DRV8835). To support future autonomous operation, the board also has an accelerometer (IIS328DQTR), IR transceivers for robot-robot communication (EK8460 and VS1838B), and a color sensor for localizing against a colored backdrop (TCS34725).

A. Granular Material

The performance of the robot is closely tied with the properties of the granules that make up its environment. While the mechanics of granular media in the "frictional fluid" regime are increasingly well understood from experimental,

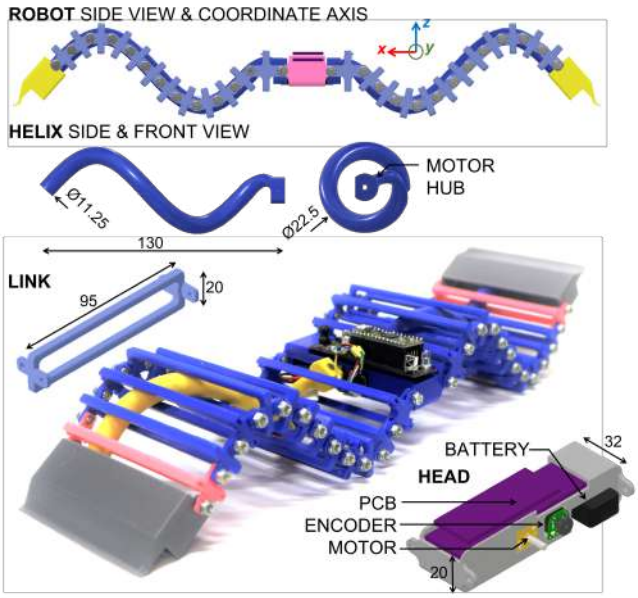

Figure 2. Robot design. Dimension: $383\times62\times101\text{mm}^3$. Weight: 283g.

exact simulation (multiparticle discrete element method and continuum models), and approximate models (resistive force theory, RFT) [21], [22], [23], [24], [25], [26], [27], [28], [29] we opted for a physical ("robophysics" [**?**], [30]) approach to study the performance and discover novel mechanics during robot movement on and within the medium. This is rationalized by the fact that simulation of irregularly shaped grains can be time consuming [31], continuum models might not yet apply, and RFT parameters are not available for our medium. How to optimize the robot design parameters according to the size, weight, and shape of the granules is thus an interesting study beyond the scope of this article.

Because our robot has a small form factor, low weight, low-power motors, and a relatively open profile in which small granules may get caught, it is restricted to interaction with large, light weight granules. We compared two types of anti-static, bio-degradable packing peanuts which are inexpensive and easy to come by. Specifically, we examined cylindrical straight and curved profile peanuts from Secure Seal. The straight peanuts are 50mm long, 16mm diameter, and weigh 0.19g; the curved peanuts have an arc of 90^o, a 26mm curvature radius, 16mm diameter, and weigh 0.16g.

Curved peanuts entangle more than straight peanuts, which make them better suited for construction, akin to wet versus dry sand. Entanglement is advantageous for assembly because it can produce high strength-to-weight ratio without binders, and can support self-healing and continuous forms [32], [33], [34], [35]. We compared the capabilities of the two types of peanuts (straight vs curved) to support shear stresses by performing two tests. The first was a "drop test" [36] in which we released a 75mm diameter 1m long tube of peanuts onto the ground 10 times. This showed that curved peanuts are more structurally stable than straight peanuts: the average height of the mounds created was 125 ± 14mm for curved versus 104 ± 8mm for straight peanuts, and the mound slopes were 37 ± 11um/mm

for curved and 26±7um/mm for straight peanuts. We also performed "avalanche tests" [37] in which we glued a single layer of peanuts onto a 150×350mm box with an open end, covered it in a 4-5 loose granule layer and tilted the box until the peanuts rolled off, 10 times. Again, we found that curved entangle better than straight peanuts; peanuts generally started rolling off beyond 15^o, but full avalanche occurred at 40 ± 4^o for curved and 32 ± 2^o for straight peanuts.

B. Experimental Setup

Based on Sec. II-A, all further robot characterization was done with curved packing peanuts. To evaluate robot performance, we set up vertical aquariums partially filled with these granules at a depth of at least 180mm to avoid influence from solid ground. To confine the robots to planar motion, the aquarium width is 114mm, slightly wider than the robot. All evaluations are based on videos and images from a side-view camera and automated image processing. To produce a quantitative estimate of material movement dependent on robot behavior, the software thresholds the white packing peanuts against the darker robot and background.

Values reported are the average result of 5 trials, done with tethered, manually controlled robots unless otherwise noted. Tethered robots permit longer trials without concern for battery life, and exploration of behaviors that otherwise require more advanced sensor feedback. We found that tethered and untethered robots behave similarly, albeit with slight adjustments to the number of helix rotations within control sequences, likely due to the 25g weight difference.

C. Robot Locomotion

The robot moves best on or close to the ground, where the material compresses less. The maximum velocity on ground and on a flat layer of granules was recorded as 96mm/s±9mm/s and 67mm/s±5mm/s, respectively (Fig. 3). As expected, performance is independent of direction, and the robot moves slower on granules than on ground. We found that a robot could climb granular inclines up to 30% with an average speed of 36mm/s±18mm/s. At steeper slopes, the robot starts shifting granules downwards and eventually becomes stuck.

We measured the untethered robot payload by having it move at full speed on level ground, and then pressing a scale onto its head. At 1.6kg the gear broke - that is the robot has a payload of at least 5.8 times its own weight, leaving plenty of overhead for batteries and drivers. With the current battery, the untethered robots are able to move 25m over flat granules on a single charge (duration ∼6.3 min). We estimated robot traction on granules by having the untethered robot push against a scale for 30s and measuring the readout at 10fps. The mean pushing force of the robot was 0.54±0.3N corresponding to ∼300 peanuts. However, it is worth noting that because the robot-granule interaction causes granule compaction over time, the pushing force doubles from the first 5s to the last 5s of the trial. As discussed later, the pushing force may be increased by adding weight to the robot. Finally, we measured the Cost of Transport on flat ground ($\text{COT} = P/(mgV_{ave})$) to be approximately 7.9, approximately twice that of previous single-tailed design iterations of the SAW mechanism (COT = 3.8) [19].

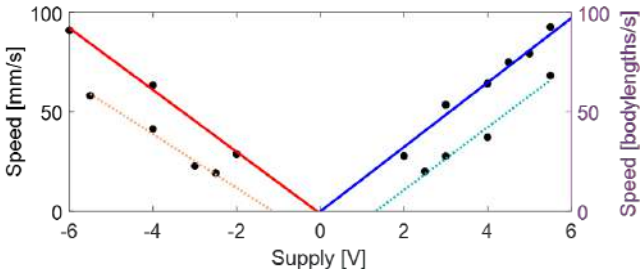

Figure 3. Robot speed on flat ground (solid lines) and granules (dotted lines) versus supply voltage, V_s. Black marks data points; solid blue and cyan best fit lines for $+V_s$, and solid red and orange lines for $-V_s$.

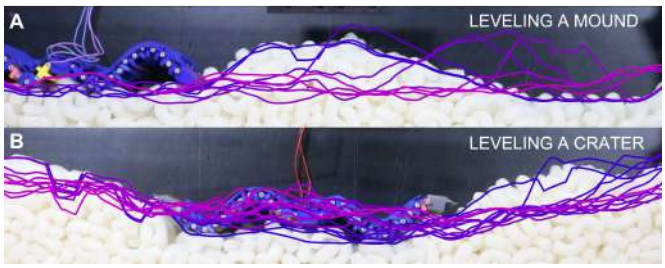

Figure 4. Two leveling challenges, blue through pink curves show the granular surface over time. A. The robot first pushes the mound right, then evens out the protrusion by moving back left. B. The robot first levels out the right slope of the crater, then repeats the process on the left.

III. Interaction with Granular Media

We next describe and characterize action sequences that allow a single double-tailed SAW robot to level, subtract, construct, and transport material.

Leveling: The ability to level a surface is critical to generate building foundations and access paths for less agile machinery. We tested mound and crater leveling. For the former, the robot climbs up the slope and then drives both tails inwards, causing the granules on the mound to be pushed outwards. For the latter, the robot slowly climbs up the slope, and then alternately anchors one tail while driving the other forwards to push granules back into the crater.

When leveling a mound similar to the robot size (Fig. 4.A), the maximum height difference of the terrain was lowered by 47%±20%. Note, that the maximum difference was affected by the fact that the robot cannot easily lower the height of granules near the aquarium edge. The video further shows an untethered robot leveling a mound its own width and ∼3 times its height using the same control sequence. When leveling a similar-sized crater (Fig. 4.B), the maximum terrain height difference was lowered by 48%±9.9%.

After leveling, the maximum difference in surface height was ∼60% of the robot height. Provided the incline is <30%, we have not found limits on what can be leveled.

Subtraction: To create a crater from level ground, a robot drives its tails in opposing directions, shifting granules out from underneath itself while staying still. Our tethered robot

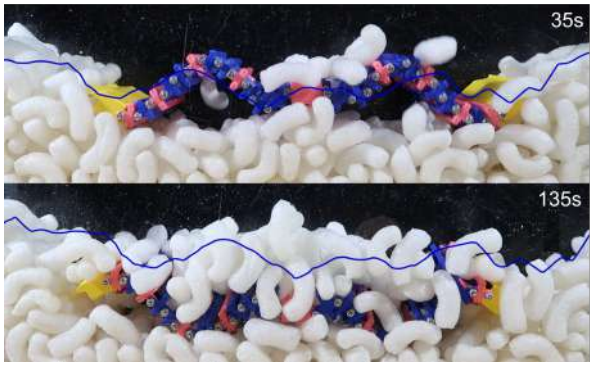

Figure 5. Indentation and later submerging by an untethered robot, starting from a level surface (outline shown in blue).

can dig a hole its own depth in 60s; the heavier untethered robot can dig the same hole in ∼35s. When the robot continues to dig, it eventually submerges until stabilizing just under the surface (Fig. 5).

Addition: A robot can scrape material off a level surface to construct a mound. It does this by sequentially anchoring the posterior tail and driving the anterior tail outwards, then moving forward and repeating this behavior to create a mound in front. A tethered robot can accumulate a mound roughly half its own size (∼0.0019m^3) in ∼96s±18s by scraping off granules over 0.38m; we found similar results in a single trial with an untethered robot.

Transport: The ability to transport material on or off the site is important to construction systems. Here, we examine three ways to transport material: 1) by pushing material in front of the robot, 2) by carrying it on the robot back, and 3) by shuffling material along the length of the robot in a conveyor belt-like fashion. The first may be especially useful to build mounds; the second to transport material between construction sites; and the last may enable robots to form a bucket-brigade to collectively move material.

To push a mound of material, the robot slowly climbs onto the side of the mound, then anchors the posterior tail and drives the anterior tail inwards effectively pushing granules forward (Fig. 6.A-B). The robot can move ∼0.0014m^3 0.60m in 180s. As mounds are moved there is waste, as an example Fig. 6.C shows how granules fall off the mound after ∼110s. Over 5 trials, moving ∼0.0018m^3 a distance of 0.60m, we found that the mound decreased in size by 31%±15%. To carry material, the robot simply moves forward. On granules, the robot can move 0.0019m^3 0.50m in 32s, with an average loss of ∼27% ± 18% (Fig. 6.E). To shuffle material along the length of the body, the robot alternately anchors one tail while slowly moving the other forward (Fig. 6.F).

IV. Multi-Robot Interaction

The robot design is optimized for collaborative motion: robots can climb onto and over each other, and even help push each other up inclines and into granules. The former enables many robots to work in the same space, and allows robots to stack, effectively increasing their mass to create a greater impact on the granules. In the following subsections, we characterize the ability of robots to climb on each other, construct, and burrow.

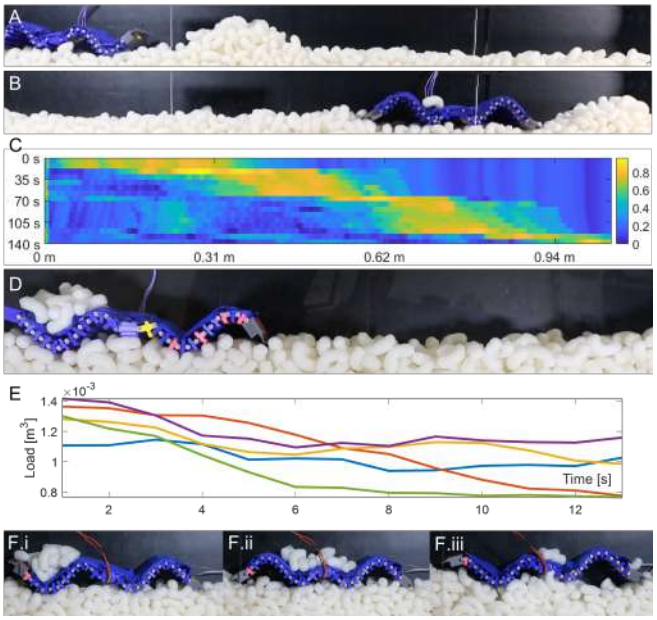

Figure 6. A-B. Snapshots before and after moving a mound. C. Data from a single trial, showing the position of granules over time (the color denotes the fraction of image height per column in the frame, cropped just under the level surface). D-E. Snapshot of a robot transporting granules and load volume over time. F.i-iii. Snapshots as robot stays in place while moving granules along the length of its body.

Collaborative Motion: We found that both tethered and untethered robots could reliably climb onto and past each other while moving in opposite directions (Fig. 7.A). In 10 trials with tethered robots, the passing took 18.6s±2.2s, and the top robot experienced a tenfold speed reduction (∼8.6mm/s); whereas the bottom experienced a threefold speed reduction (∼21mm/s). This insight might be important for passages between robots of different power levels or priorities in future autonomous systems.

A robot can also climb under another robot that is moving in place (with tails moving in opposing directions) successfully in 8 out of 10 trials. This indicates that one robot can help another robot become unstuck, e.g. at the bottom of a steep hill, or to climb steeper obstacles than is possible on its own. Fig. 7.B shows one robot pushing another up a 60% slope, albeit causing erosion by ∼20^o.

Collaborative Construction: The low weight of a single robot means that it can navigate granules with little impact. However, with the ability of robots to climb onto each other, two stacked robots moving forward in synchrony press deep enough into the surface to accumulate granules forwards, effectively constructing mounds (Fig. 7.C). Two robots moving over 0.38m can construct a mound 0.0019m^3 in 8s – i.e. $1/10$th of the time it takes a single robot. Moreover, with two robots, this process does not require feedback control to work well. The accompanying video further shows two robots collaboratively building a ramp to climb a discrete step in the terrain.

Collaborative Burrowing: Although a single robot does not have sufficient dexterity or traction to burrow into granules,

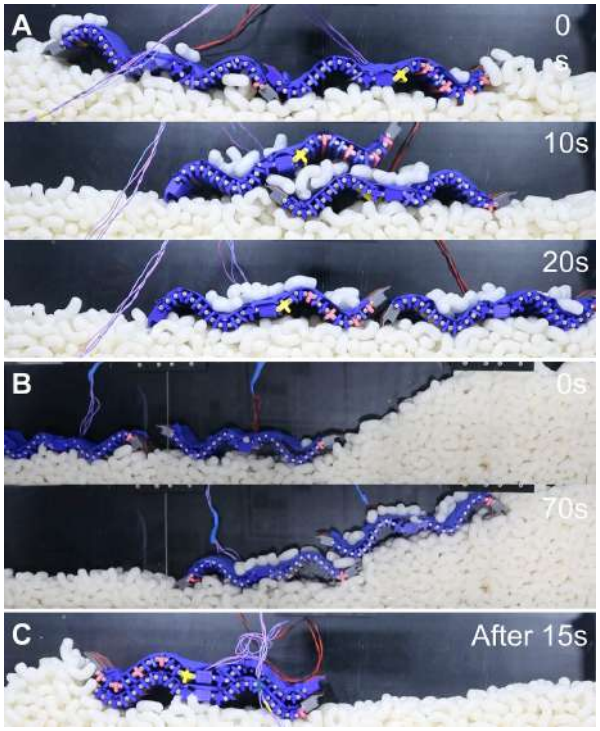

Figure 7. A. Two robots passing each other. B. Robot helping another climb a 60% slope. C. Stacked robots moving in synchrony accumulate material in their direction of motion.

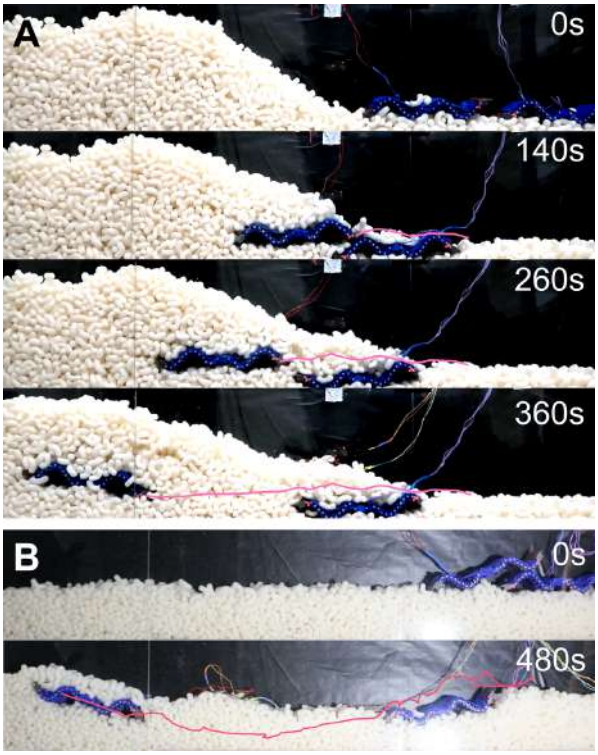

Figure 8. Snapshots of collaborative burrowing sideways (A) and down (B) into granules; visually tracked path (smoothed over 15s) of the burrowing robot is overlaid in pink.

one robot can help another burrow (Fig. 8). Collaborative burrowing is accomplished by having the first robot move under the second, angling it downwards by an amount corresponding to the overlap between the robots. The second robot now moves slowly forward in synchrony with the first robot and uses the friction to the surface of the first robot to locomote forwards into the granules. It is interesting to note that 1) when the second robot is fully embedded in the granules, it no longer needs the first robot to help, and 2) as the second robot has no way to produce downwards force, it eventually resurfaces from the granules. This phenomenon is described more in [7]. The ability of multiple robots to shift each other downwards, yet resurface automatically may be of interest to future burrowing applications, such as minimally invasive subterranean cable or sensor placement.

V. Pathways to Autonomy and Extension to 3D

In summary, we found that compaction, mound-leveling, subtraction, some types of transport, and collaborative motion work with fixed, open-loop action sequences. Cooperating those findings, we demonstrated compaction, mound-leveling, addition and two robots climbing over each other using untethered robots using only encoders as feedback. To level a crater and to move a mound, robots will need to locate the incline with an accelerometer. To burrow, encoders may further help position the tail cap downwards. To do collaborative construction and burrowing, the robots will need to sense their relative distance and phase offsets. For higher-level construction tasks, robots may benefit from localization. Note, that the untethered robot already houses all of these sensors, demonstrating that they physically fit in the same form factor. In the future, we hope to demonstrate closed loop control and plans that incorporate the inherent interaction of the robot and surface. In addition, principles from entangled active agents (worm and smarticle robot blobs) could be of value in collective task completion [38].

There are many pathways to 3D operation, e.g. we could add an actuated link between the two helices as in [20] or place two SAWs side by side to accomplish skid-like steering. Because our interest is in minimalistic robot-granule interactions and because our mechanism is robust to physical perturbations, we instead propose to generate the third DOF via collisions between robots with intersecting trajectories. Given a sufficient density of robots, this method will in theory be guaranteed to eventually cover the entire space. To exemplify such interactions, we used T-bone collisions of various lengths between two robots to achieve heading changes of $[6^o, 9^o, 11^o, 26^o, 31^o]$ (see video).

VI. Mechanical considerations

Our experiments indicate that the SAW mechanism can be improved. In particular, we aim to minimize mechanism dissipation due to frictional sliding between parts, or worst case friction that locks the mechanism entirely. Sliding between parts, however, is intrinsic to the mechanism design therefore the general goal must be to reduce the normal forces at points of sliding. To aid discussion, take the x direction to be from the motor base out in the direction of the helix axis, y along the slats that make up the links, and z up orthogonal to the wavy plane defined by the slats (Fig. 2)

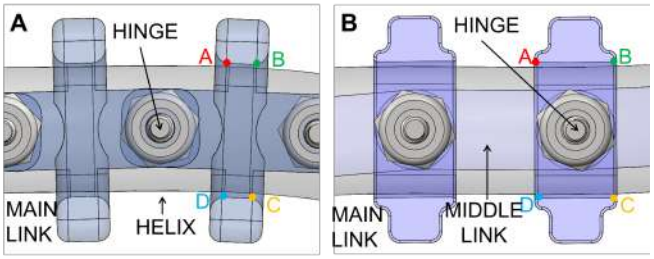

Figure 9. A. Present design, link on the helix. The helix progression rotates the link by forces at B and D or at A and C. Because hinges are not in the middle of the link, link interaction can cause moments. B. Proposed link design, where 1) the contact distance, w, (AB or CD) has a larger moment on the link from a given normal contact force, and 2) buckling from compression in the chain is inhibited.

As described in detail in [19], the basic mechanism is a rectangular chain that surrounds a helix. As the helix rotates on its axis the chain is forced to undulate sinusoidally and, most importantly, the links are each forced to rotate. It is the rotation of the links, at the maximum and minimum of the sine wave which drives the robot forwards on dry material. The issues here, involving link details, are somewhat different than the general screw-drive considerations in [8].

Some sliding is intrinsic to the mechanism and unavoidable: 1) Link-helix sliding; this sliding is almost exactly in the y direction. 2) Link-link sliding at their hinges; this includes bearing friction at the pins and sliding of one hinge surface on the next to which it is pinned. Obviously, friction can be reduced if low friction materials are chosen. For a given set of materials, however, we next discuss design and usage details that induce (non-essential) normal contact forces and consequently the friction forces and dissipation.

a) Torques caused by the helix-to-link contact being off center: One might expect large friction at the link joints from torques due to the helix mostly being off center (y direction) on the link. However, chain twist is resisted by the two joints in each link which are separated by a large distance in the y direction, causing little out-of-plane torque to be resisted by the individual joints. Holding the rectangular chain in our hands without the helix, we could not induce notable friction at the link-to-link joints, even when the chain was twisted, so we drop that as an issue.

b) Link normal forces and drive forces: The drive force comes from frictional contact between the bottom of a link and the substrate. The useful work is the foot's distance of motion, relative to the mechanism, times the force. At one link, this force is generated by torque from contact between the link and the helix, at AC or BD (Fig. 9.A). This torque only generates useful force because of resistance to motion at the hinge. That is, the propulsive force is, at least in part, reacted by tension or compression in the chain at the link-to-link hinges. Working down the chain, this drives the whole mechanism. The helix itself also adds to the drive similar to a screw drive, with the notable difference that the helix (or screw) is driving into material that is part of the machine rather than part of the substrate. The normal force at the contact points $ABCD$ could be reduced if the widths AB and CD were increased, as shown in Fig. 9.B. Further, the tendency for frictional jamming, of each link on the helix, is reduced by increasing the lengths AB and CD.

c) Buckling: A chain of links buckles under compression. When the wave travels inwards, the mechanism chain is in compression and partially folds around the helix, back and forth. This buckling is resisted by normal forces at points $ABCD$ which is not useful for locomotion and induces parasitic friction. This buckling effect could be reduced by the two design changes illustrated in Fig. 9.B: The width AB=CD could be increased (as also suggested above), and the gap between the link and the helix could be reduced to the minimum allowed by the curvature of the helix. The ability to keep a small gap is enhanced if the helix has a round cross section in planes orthogonal to the x axis (rather than orthogonal to the helix curve). In initial trials of this design, we found that because the two sets of middle links on either side of the robot were no longer fixed on the main links or to each other, they were free to create considerable twist around the x-axis. We conclude that this design extension would require each chain to be driven by two side-by-side, mirrored helices to prevent out-of-plane twist.

d) Curvature-induced normal forces: The chain is in tension, or compression, due to the drive forces at ground-link contact. This tension (or compression) induces a normal force (per unit length) on the helix proportional to the amount of tension, or compression, and the helix curvature. This normal force, and the consequent friction, are unavoidable.

e) End effects: Occasionally we saw jamming at the head link. We think such effects are due to an incompatibility between the motions allowed by the planar link mechanism (in the xy plane) and those prescribed by the planar projection of the helix. At present, our helices taper off center, and the first chain hinge is not located at the taper point. Therefore, the problem may be eliminated if the helix tapers to a point on the motor axis and the first hinge of the chain, mounted to the robot body, has an axis through that point.

VII. Conclusion

We introduced a double-tailed SAW robot that enables an unprecedented multitude of construction behaviors in a single system. The approach stands in contrast to prior related literature both for its minimalism (motion and manipulation are achieved in the same 2-DOF mechanism), and by the fact that it relies on collaborative physical interactions between robots. Beyond modifying the surface according to a particular shape or functionality, the robots may also leverage the granules to extend their own workspace (see Video).

The scope of this paper was limited to manual- and open-loop controlled robots operating in 2D aquariums filled loosely with packing peanuts. Towards future autonomy, we showed that drivers, batteries, and sensors practically fit on an untethered robot, and that open-loop control often suffices. Finally, we discussed forces acting on the mechanism and options for improvement. Whether these, and more, will make it feasible to scale this mechanism to real-world granular materials is an open question left for future work.

REFERENCES

[1] K. H. Petersen, N. Napp, R. Stuart-Smith, D. Rus, and M. Kovac, "A review of collective robotic construction," *Science Robotics*, vol. 4, no. 28, 2019.

[2] I. A. Davydychev, J. T. Karras, and K. C. Carpenter, "Design of a two-wheeled rover with sprawl ability and metal brush traction," *Journal of Mechanisms and Robotics*, vol. 11, no. 3, p. 035002, 2019.

[3] V. Thangavelu, M. S. da Silva, J. Choi, and N. Napp, "Autonomous modification of unstructured environments with found material," in *2020 IEEE International Conference on Robotics and Automation (ICRA)*. IEEE, 2020, pp. 7798–7804.

[4] C. Li, P. B. Umbanhowar, H. Komsuoglu, D. E. Koditschek, and D. I. Goldman, "Sensitive dependence of the motion of a legged robot on granular media," *Proceedings of the National Academy of Sciences*, vol. 106, no. 9, pp. 3029–3034, 2009.

[5] J. De la Fuente, R. Shor, and S. Larter, "Single actuator peristaltic robot for subsurface exploration and device emplacement," in *2020 IEEE International Conference on Robotics and Automation (ICRA)*. IEEE, 2020, pp. 8096–8102.

[6] M. M. Coad, L. H. Blumenschein, S. Cutler, J. A. R. Zepeda, N. D. Naclerio, H. El-Hussieny, U. Mehmood, J.-H. Ryu, E. W. Hawkes, and A. M. Okamura, "Vine robots: Design, teleoperation, and deployment for navigation and exploration," *IEEE Robotics & Automation Magazine*, vol. 27, pp. 120–132, 2019.

[7] N. D. Naclerio, A. Karsai, M. Murray-Cooper, Y. Ozkan-Aydin, E. Aydin, D. I. Goldman, and E. W. Hawkes, "Controlling subterranean forces enables a fast, steerable, burrowing soft robot," *Science Robotics*, vol. 6, no. 55, 2021.

[8] T. Dachlika and D. Zarrouk, "Mechanics of locomotion of a double screw crawling robot," *Mechanism and Machine Theory*, vol. 153, p. 104010, 2020.

[9] M. Green, T. McBryan, D. Mick, D. Nelson, and H. Marvi, "Regolith excavation performance of a screw-propelled vehicle," *Advanced Intelligent Systems*, p. 2100125, 2021.

[10] K. Skonieczny, M. E. DiGioia, R. L. Barsa, D. S. Wettergreen, and W. L. Whittaker, "Configuring innovative regolith moving techniques for lunar outposts," in *2009 IEEE Aerospace conference*. IEEE, 2009, pp. 1–11.

[11] R. P. Mueller, R. E. Cox, T. Ebert, J. D. Smith, J. M. Schuler, and A. J. Nick, "Regolith advanced surface systems operations robot (rassor)," in *2013 IEEE Aerospace Conference*. IEEE, 2013, pp. 1–12.

[12] K. Dierichs, O. Kyjánek, M. Loučka, and A. Menges, "Construction robotics for designed granular materials: in situ construction with designed granular materials at full architectural scale using a cable-driven parallel robot," *Construction Robotics*, vol. 3, no. 1, pp. 41–52, 2019.

[13] D. Monaenkova, N. Gravish, G. Rodriguez, R. Kutner, M. A. Goodisman, and D. I. Goldman, "Behavioral and mechanical determinants of collective subsurface nest excavation," *The Journal of experimental biology*, vol. 218, no. 9, pp. 1295–1305, 2015.

[14] I. Hurkxkens, D. Pigram, and J. Melsom, "Shifting sands: Experimental robotic earth-moving strategies in dynamic coastal environments," *Journal of Digital Landscape Architecture*, pp. 66–74, 2021.

[15] C. Schenck, J. Tompson, S. Levine, and D. Fox, "Learning robotic manipulation of granular media," in *Conference on Robot Learning*. PMLR, 2017, pp. 239–248.

[16] W. Kim, C. Pavlov, and A. M. Johnson, "Developing a simple model for sand-tool interaction and autonomously shaping sand," *arXiv preprint arXiv:1908.02745*, 2019.

[17] J. Aguilar, D. Monaenkova, V. Linevich, W. Savoie, B. Dutta, H.-S. Kuan, M. Betterton, M. Goodisman, and D. Goldman, "Collective clog control: Optimizing traffic flow in confined biological and robophysical excavation," *Science*, vol. 361, no. 6403, pp. 672–677, 2018.

[18] K. Petersen and R. Nagpal, "Complex design by simple robots: A collective embodied intelligence approach to construction," *Architectural Design*, vol. 87, no. 4, pp. 44–49, 2017.

[19] D. Zarrouk, M. Mann, N. Degani, T. Yehuda, N. Jarbi, and A. Hess, "Single actuator wave-like robot (saw): design, modeling, and experiments," *Bioinspiration & biomimetics*, vol. 11, no. 4, p. 046004, 2016.

[20] D. Shachaf, O. Inbar, and D. Zarrouk, "Rsaw, a highly reconfigurable wave robot: Analysis, design, and experiments," *IEEE Robotics and Automation Letters*, vol. 4, no. 4, pp. 4475–4482, 2019.

[21] P. E. Schiebel, H. C. Astley, J. M. Rieser, S. Agarwal, C. Hubicki, A. M. Hubbard, K. Diaz, J. R. Mendelson III, K. Kamrin, and D. I. Goldman, "Mitigating memory effects during undulatory locomotion on hysteretic materials," *Elife*, vol. 9, p. e51412, 2020.

[22] S. Agarwal, A. Karsai, D. I. Goldman, and K. Kamrin, "Surprising simplicity in the modeling of dynamic granular intrusion," *Science Advances*, vol. 7, no. 17, p. eabe0631, 2021.

[23] ——, "Efficacy of simple continuum models for diverse granular intrusions," *Soft Matter*, vol. 17, pp. 7196–7209, 2021. [Online]. Available: http://dx.doi.org/10.1039/D1SM00130B

[24] T. Zhang and D. I. Goldman, "The effectiveness of resistive force theory in granular locomotion," *Physics of Fluids*, vol. 26, no. 10, p. 101308, 2014.

[25] J. Aguilar and D. I. Goldman, "Robophysical study of jumping dynamics on granular media," *Nature Physics*, vol. 12, no. 3, pp. 278–283, 2016.

[26] C. Li, T. Zhang, and D. I. Goldman, "A terradynamics of legged locomotion on granular media," *science*, vol. 339, no. 6126, pp. 1408–1412, 2013.

[27] Y. Ding, S. S. Sharpe, A. Masse, and D. I. Goldman, "Mechanics of undulatory swimming in a frictional fluid," *PLoS computational biology*, vol. 8, no. 12, p. e1002810, 2012.

[28] Y. Ding, N. Gravish, and D. I. Goldman, "Drag induced lift in granular media," *Physical review letters*, vol. 106, no. 2, p. 028001, 2011.

[29] R. D. Maladen, Y. Ding, C. Li, and D. I. Goldman, "Undulatory swimming in sand: subsurface locomotion of the sandfish lizard," *science*, vol. 325, no. 5938, pp. 314–318, 2009.

[30] Y. O. Aydin, J. M. Rieser, C. M. Hubicki, W. Savoie, and D. I. Goldman, "Physics approaches to natural locomotion: Every robot is an experiment," in *Robotic Systems and Autonomous Platforms*. Elsevier, 2019, pp. 109–127.

[31] S. Zhao, N. Zhang, X. Zhou, and L. Zhang, "Particle shape effects on fabric of granular random packing," *Powder technology*, vol. 310, pp. 175–186, 2017.

[32] K. Dierichs and A. Menges, "Granular construction: Designed particles for macro-scale architectural structures," *Architectural Design*, vol. 87, no. 4, pp. 88–93, 2017.

[33] N. Gravish, S. V. Franklin, D. L. Hu, and D. I. Goldman, "Entangled granular media," *Physical review letters*, vol. 108, no. 20, p. 208001, 2012.

[34] D. Hu, S. Phonekeo, E. Altshuler, and F. Brochard-Wyart, "Entangled active matter: From cells to ants," *The European Physical Journal Special Topics*, vol. 225, no. 4, pp. 629–649, 2016.

[35] D. Andreen, P. Jenning, N. Napp, and K. Petersen, "Emergent structures assembled by large swarms of simple robots," 2016.

[36] R. D. Maladen, Y. Ding, P. B. Umbanhowar, and D. I. Goldman, "Undulatory swimming in sand: experimental and simulation studies of a robotic sandfish," *The International Journal of Robotics Research*, vol. 30, no. 7, pp. 793–805, 2011.

[37] O. Pouliquen and Y. Forterre, "Flows of dense granular media," *Annual Review of Fluid Mechanics*, vol. 40, pp. 1–24, 2008.

[38] Y. Ozkan-Aydin, D. I. Goldman, and M. S. Bhamla, "Collective dynamics in entangled worm and robot blobs," *Proceedings of the National Academy of Sciences*, vol. 118, no. 6, 2021.